Investigation of the Effect of Chromium Replacing with Cerium in Magnesium Ferrite on the Dielectric and Structural Properties

Hamed A. Younis[1,*], Wissam A. Hussian[1,†], Omar A. Ahmed[1,‡], Mustafa H. Omar[2,§]

[1] *The General Directorate for Education in Diyala, Diyala, Iraq*
[2] *Department of Materials Engineering, College of Engineering, University of Diyala, Diyala, Iraq*

The structural and dielectric properties of cerium-chromium substitution in magnesium ferrite ($x = 0$, 0.1, 0.3, 0.5) prepared by spontaneous combustion of citric acid and calcined at a temperature of (1000 °C) were studied. The compositional characterization of the samples was carried out using XRD, FTIR, TEM, and the dielectric properties were measured using LCR. X-ray diffraction revealed the composition of the cubic spinel. The crystal size of magnesium ferrite was within (18-31 nm) and the lattice constant (8.327-8.393 Å). It was observed that the FTIR spectra of the compound $MgCr_{0.5-x}Ce_xFe_{1.5}O_4$ remained in the spinel phase with a change in the concentration of Ce^{3+}. Electron microscopy measurements showed that there are different lattice tips with potential d-spacing for Cr_2O_3, CeO_2 and α-Fe_2O_3 phases. The d-spacing value of the most prominent ring in the (311) crystal planes of $MgFe_2O_4$ was close to its value in X-ray diffraction. It was found that the dielectric constant and the dielectric loss coefficient decreased with the increment in the frequency of the applied electric field and the alternating conductivity.

Keywords: $MgFe_2O_4$, Dielectric properties, Sol-Gel, TEM, FTIR.

1. INTRODUCTION

Recently, technological development required obtaining high-performance devices through synthesis processes in spinel-type Nano ferrites for ease of preparation and distinctive properties. And multi-field applications, including high-frequency operating devices, switching, wastewater treatment, drug delivery, and magnetic hyperthermia applications. The method of preparation and the additives affect the distribution of the cation and this is reflected on the properties of ferrite [1, 2]. The sol-gel spontaneous combustion method used in this study is characterized by producing a highly homogeneous crystalline material with low temperature, low cost and short time [3].

In a face-centered cubic structure, the spinel type ferrite crystallizes. This type is classified into normal, inverted and mixed based on how the divalent and trivalent metal ions are distributed throughout the octahedral and tetrahedral cations locations [4-6]. Magnesium ferrite $MgFe_2O_4$ is a natural spinel type and can be described as an n-type semiconductor having a small bandgap of 1.9 eV [7]. Trivalent iron cations can be replaced by a small amount of other cations of slightly larger size than the ferrous cations, but become undesirable when rare earth (RE) cations of larger size such as Ce^{3+} (1.143 Å) are added. This certainly affects the crystal structure of spinel and causes several changes in the electrical and structural characteristic due to the distortion caused by rare earth cations in the crystal structure and the occurrence of a RE-Fe super exchange reaction [8-10]. Such studies found importance in the applications of antibacterial properties, improve catalysis, memory storage, magnetic fluids,

and apoptosis [8, 11].

During this study, it was found that the replacement of cerium cations (Ce^{3+}) with chromium cations (Cr^{3+}) in the compound $MgCr_{0.5-x}Ce_xFe_{1.5}O_4$ ($x = 0$, 0.1, 0.3, 0.5) It caused a change in the structural and electrical properties during cations exchange and exchange reactions.

2. EXPERIMENTAL WORK

The composite $MgCr_{0.5-x}Ce_xFe_{1.5}O_4$ ($x = 0$, 0.1, 0.3, 0.5) was made by the citrate-gel spontaneous combustion technique, from magnesium nitrate, chromium nitrate, cerium nitrate and citric acid as raw materials.

By dissolving the required quantities of citric acid and metal nitrate in a ratio of 3:1 separately in a proper amount of distilled water. By combining the solutions with a magnetic stirrer, a homogeneous solution was obtained. Then by adding ammonia, the pH of the combined solution is raised to 7. The temperature is raised to 100 °C with continuous stirring a dense gel was produced after evaporating the solution. The gel is dried and self-fired inside an oven at 250 °C subsequently ferrite powder was acquired. The resulting powder was grounded and sintered at 1000 °C for 4 hours.

3. RESULTS AND DISCUSSION

3.1 Structural Characterization

XRD- analysis was performed at 30 °C. Fig. 1 show formation of the cubic spinel structure for synthesis $MgCr_{0.5-x}Ce_xFe_{1.5}O_4$ ($x = 0$, 0.1, 0.3, 0.5) which belong

* Hamedabd925@gmail.com
† Wissamyass1979@gmail.com
‡ Omarphy50@gmail.com
§ Mustafahassan550@gmail.com

to the space group Fd3m. The compound has been identified by JCPDS Card No. 36-0398) in addition to presence of other secondary phases like Cr_2O_3, CeO_2 and Fe_2O_3. It was found that the peak (311) in the structure of spinel decreases by adding of Cerium against the decrease of chromium. The crystal size of (D) $MgCr_{0.5-x}Ce_xFe_{1.5}O_4$ Nano ferrites was calculated using the maximum peak intensity (311) of the Scherer formula.

It is shown in Table 1. that the lattice parameter of the ferrite compound $MgCr_{0.5-x}Ce_xFe_{1.5}O_4$ increases with the increase in Cerium content due to the different ionic radii, the ionic radius of cerium (1.143 Å) is larger than that of chromium (0.63 Å), which causes Lattice dimensionality expansion in spinel assembly structure [9].

Table 1 – Shows experimental lattice constant (a), crystallite size (D)] for $MgCr_{0.5-x}Ce_xFe_{1.5}O_4$

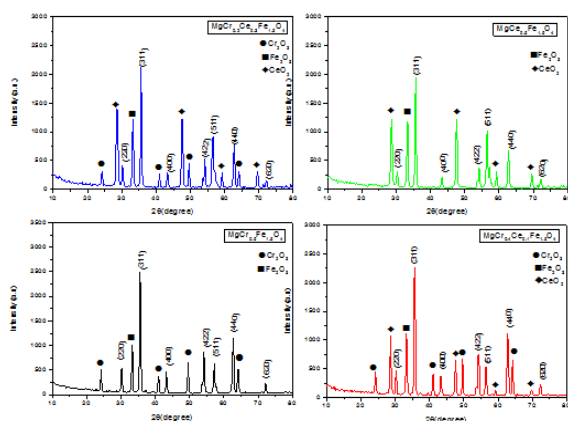| Composition	Content (X)	Lattice parameter a (Å)	Crystallite size D (nm)
$MgCr_{0.5}Fe_{1.5}O_4$	0.0	8.327	18
$MgCr_{0.4}Ce_{0.1}Fe_{1.5}O_4$	0.1	8.341	23
$MgCr_{0.3}Ce_{0.2}Fe_{1.5}O_4$	0.3	8.375	26
$MgCe_{0.5}Fe_{1.5}O_4$	0.5	8.393	31

Fig. 1 – XRD patterns $MgCr_{0.5-x}Ce_xFe_{1.5}O_4$ ($x = 0, 0.1, 0.3, 0.5$)

3.2 FT-IR Analysis

Infrared spectroscopy is a technique that relies on the absorption of electromagnetic radiation to determine the sites of bonds and to identify the structure and redistribution of cations between sites. The FTIR spectroscopy within the range (400-4000 cm^{-1}) of the samples prepared for the calcined compound $MgCr_{0.5-x}Ce_xFe_{1.5}O_4$ ($x = 0, 0.1, 0.3, 0.5$) at a temperature (1000 °C) possess expansion vibrations in two locations of the metal atom with oxygen according to the geometry of the nearest neighbors are shown in Fig. 2. The vibration of the metal atom with the oxygen in the tetrahedral sites within the range (536.2 – 519.34 cm^{-1}) while in the octahedral sites (431.78 – 414.48 cm^{-1}). The normal state of bond vibration in tetrahedral sites (Th) is higher than in octahedral sites (Oh) because the bond length in tetrahedral sites (d (MA-O) < 2 Å) is less than in octahedral sites (d (MB-O) > 2 Å). Fig. 2 shows the FTIR spectra of the complex ($MgCr_{0.5-x}Ce_xFe_{1.5}O_4$) it remains in the spinel phase with a change in the concentration of Ce^{3+}, that the change in the vibrations of the two sites is due to the redistribution of the cations of the metal ions, additionally to the metals' varying ionic radii [12–14].

3.3 TEM Morphological Observations

The HR-TEM images of the samples ($x = 0.0, 0.5$) are inset with the corresponding area electron diffraction (SAED) patterns in Fig. 2. The rings' ordering of SAED spots showed the crystal structure of magnesium ferrite.
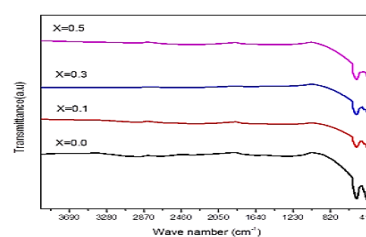

Fig. 2 – FTIR- spectra of $MgCr_{0.5-x}Ce_xFe_{1.5}O_4$ ($x = 0, 0.1, 0.3, 0.5$).

The interplanetary spacing d can be calculated from the (311)'s most noticeable ring crystal planes of $MgFe_2O_4$. Diffraction ring sizes for samples with $x = 0.0, 0.5$ were used to compute the d-spacing and the values of (0.242, 0.251) respectively The d-spacing value of the most prominent ring in the (311) crystal planes of $MgFe_2O_4$ was close to its value in X-ray diffraction. The most widespread rings of the samples ($x = 0.0, 0.5$) showed poor crystallinity and it was difficult to incorporate the Cr and Ce atoms into the structure of $MgFe_2O_4$, and this results in the growth of secondary phases that correspond to the other phases. There were different lattice fringes with possible d-spacing for the Cr_2O_3, CeO_2 and α-Fe_2O_3 phases. This coincides with the results of the XRD examination [15].
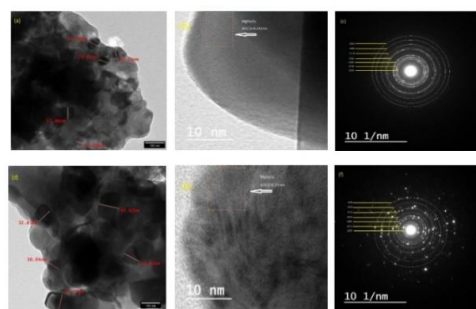

Fig. 3 – HRTEM images of $MgCr_{0.5-x}Ce_xFe_{1.5}O_4$ ($x = 0, 0.1, 0.3, 0.5$) (a-c) $x = 0.0$, (d-f) $x = 0.05$.

3.4 Dielectric Properties

The alternating conductivity, dielectric loss factor, and dielectric constant of nano-ferrite compound samples $MgCr_{0.5-x}Ce_xFe_{1.5}O_4$ were investigated at room temperature with the LCR meter in the frequency ranging from 50 Hz to 4 MHz. The changes of the dielectric constant as a function of frequency is depicted in

Fig. 4 for nano-ferrite $MgCr_{0.5-x}Ce_xFe_{1.5}O_4$ with concentrations ($x = 0.0, 0.1, 0.3$ and 0.5). It was noted that all samples possess a higher dielectric constant at low frequencies, which it quickly decreased with increasing frequency, and in ferrite materials, this is a normal tendency. The decrease in the dielectric constant was slow with increasing frequency and more stable at high frequency. This behavior in ferrites is due to the delay in the transfers of iron ions present in sites (A, B).

The phenomenon of the polarization of the space charge depends on a variation in values of the dielectric constant with frequency. It is known that the insulating material contains well-conductive particles surrounded by high-resistance grain boundaries. This space charge accumulates at the particle's edges when the electric field is applied, which has a significant impact on the value of the dielectric constant at low frequencies, and thus the voltage decreases significantly.

The electron exchange decreases as frequency increases due to the difficulty of tracking the applied electric field, so at high frequencies, the dielectric constant value approaches stability. The dielectric is dependent on electronic transitions between iron ions, granular boundaries, and oxygen empty sites [16-18].

Fe^{3+} ions shift from the A site to the B site because cerium ions prefer octahedral sites, which lowers the concentration of Fe^{3+} ions in the B site. This is why the transmission of electrons between Fe^{3+} and Fe^{2+} ions are slower, and this results in a reduction of the dielectric constant and polarization [19].

In the range of 50 Hz to 4 MHz, all samples' variations in the dielectric loss factor with respect to frequency are shown in Fig. 5 at ambient temperature. It noticed that the loss coefficient has been decreased with increasing frequency, and it is clear from the figure that the insulation loss dropped quickly in the low frequency range, but diminished progressively in the high frequency zone. The behavior can be explained through the fact that at low frequencies the resistance is high and is related to the borders of the grains, which need more energy for electron exchange (According to Koop's theory), on the contrary, the high-frequency region, which has low resistance and requires less energy to transfer electrons between iron ions in the octahedral site [19, 20].

From the Fig. 6 it noted that, the behavior of the peak called Debye relaxation when the applied electric field's frequency and the hopping frequency of the Fe^{2+} and Fe^{3+} ions match, $\omega\tau = 1$. (where ω is angular frequency and τ is relaxation time of hopping process) [21].

All samples' AC conductivities increased when the frequency increased, which is expected of ferrite. Fe^{2+} and Fe^{3+} ions are responsible for this through their electron exchange. The conductive grains are more active with increasing frequency which caused by electrons hopping between Fe^{2+} and Fe^{3+}. The more the ions, the conductivity increases and the resistance decreases. It is clear that as Mg nano ferrites and Ce contents increased, AC conductivity decreased as well. [22].

4. CONCLUSIONS

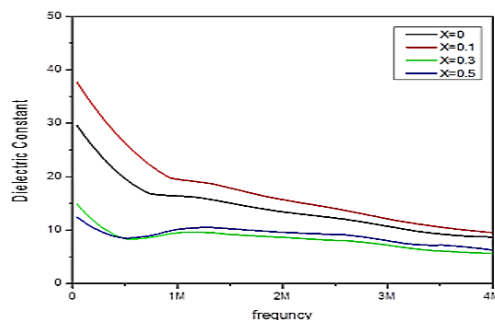Chromium was replaced by cerium in magnesium ferrite where stepwise variation of x from 0 to 0.5.

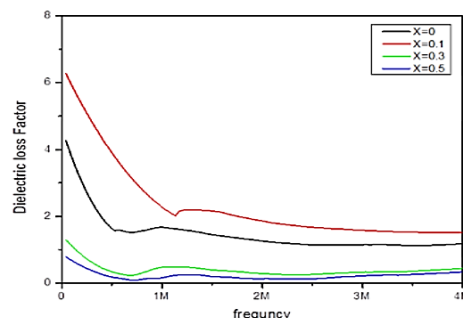**Fig. 4** – Variation of dielectric constant for $MgCr_{0.5-x}Ce_xFe_{1.5}O_4$ ($x = 0, 0.1, 0.3, 0.5$) with frequency

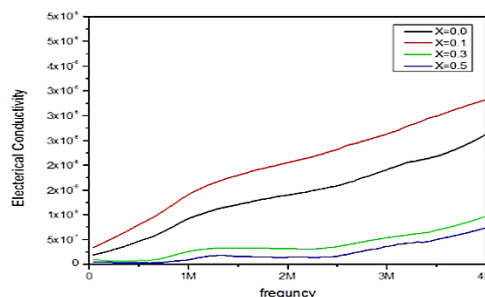**Fig. 5** – Variation of dielectric loss factor for $MgCr_{0.5-x}Ce_xFe_{1.5}O_4$ ($x = 0, 0.1, 0.3, 0.5$) with frequency

Fig. 6 – Variation of conductivity of $MgCr_{0.5-x}Ce_xFe_{1.5}O_4$ ($x = 0, 0.1, 0.3, 0.5$) with frequency

The sol-gel self-combustion process was used to prepare it. The formation of spinel ferrites with the presence of other phases (Cr_2O_3, CeO_2 and Fe_2O_3) is due to the large ionic radii of cerium and chromium compared with iron. Increasing Cerium concentration was found to increase the lattice constant and crystal size based on the analysis of X-ray diffraction data. FTIR analysis confirmed ferrite formation and redistribution of cations between A and B sites. TEM analysis showed that the size of the crystals is within the nanoscale, the crystallinity is poor, and there are different lattice fringes with possible d-spacing for the Cr_2O_3, CeO_2 and Fe_2O_3 phases. This is consistent with the XRD analysis.

The dielectric constant, dielectric loss coefficient, and alternating conductivity decreased with increasing cerium concentration in magnesium ferrite. Debye relaxation was observed after the frequency of 1M because the frequency of the ions corresponds to the frequency of the applied electric field.

REFERENCES

1. R. Zakir, S.S. Iqbal, A.U. Rehman, S. Nosheen, T.S. Ahmad, N. Ehsan, F. Inam, *Ceram. Int.* **47** No 20, 28575 (2021).
2. A.U. Rehman, N.A. Morley, N. Amin, M.I. Arshad, M.A. un Nabi, K. Mahmood, A. Ali, A. Aslam, A. Bibi, M.Z. Iqbal, F. Iqbal, N. Bano, M. Alzaid, *Ceram. Int.* **46**, 29297 (2020).
3. K. Wu, J. Li, C. Zhang, *Ceram. Int.* **45**, 11143 (2019)
4. H.R. Ebrahimi, M. Parish, G.R. Amiri, B. Bahraminejad, S. Fatahian, *J. Magn. Magn. Mater.* **414**, 55 (2016).
5. A. Šutka, K.A. Gross, *Sensor. Actuat. B Chem.* **222**, 95 (2016).
6. R. Zhang, Y. Wang, Z. Zhang, J. Cao, *Sensors (Switzerland)* **18**, 2211 (2018).
7. K. Elayakumar, A. Manikandan, A. Dinesh, K. Thanrasu, K. Kanmani Raja, R. Thilak Kumar, Y. Slimani, S.K. Jaganathan, A. Baykal, *J. Magn. Magn. Mater.* **478**, 140 (2019).
8. O.A. Ahmed, A.H. Abed, T.M. Al-Saadi, *Macromol. Symp.* **401**, 1 (2022).
9. M.A. Almessiere, Y. Slimani, A. Baykal, *J. Rare Earths.* **38**, 188 (2020).
10. M.A. Almessiere, Y. Slimani, A. Demir Korkmaz, S. Güner, A. Baykal, S.E. Shirsath, I. Ercan, P. Kögerler, *Ultrason. Sonochem.* **61**, 104836 (2020).
11. T.R. Tatarchuk, M. Bououdina, N.D. Paliychuk, I.P. Yaremiy, V.V. Moklyak, *J. Alloy. Compd.* **694**, 777 (2017).
12. B.C. Reddy, H.C. Manjunatha, Y.S. Vidya, K.N. Sridhar, U.M. Pasha, L. Seenappa, C. Mahendrakumar, B. Sadashivamurthy, N. Dhananjaya, B.M. Sankarshan, S. Krishnaveni, K.V. Sathish, P.S.D. Gupta, *J. Phys. Chem. Solids* **159**, 110260 (2021).
13. A.H. Ashour, A.I. El-Batal, M.I.A.A. Maksoud, G.S. El-Sayyad, S. Labib, E. Abdeltwab, M.M. El-Okr, *Particuology* **40**, 141 (2018).
14. P.S. Mkwae, I. Kortidis, R.E. Kroon, N. Leshabane, M. Jozela, H.C. Swart, S.S. Nkosi, *J. Mater. Res. Technol.* **9**, 16252 (2020).
15. J.C. Maxwell, *Electricity and Magnetism* (New York: 1954).
16. W.A. Yager, *The Distribution of Relaxation Times in Typical Dielectrics* (1936).
17. C.G. Koops, *Phys. Rev.* **83**, 121 (1951).
18. M. Hashim, M. Raghasudha, S.S. Meena, J. Shah, E. Sagar, S. Kumar, D. Ravinder, P. Bhatt, R.K. Kotnala, *J. Magn. Magn. Mater.* **449**, 319 (2017).
19. R. Rani, K.M. Batoo, P. Sharma, G. Anand, G. Kumar, S. Bhardwaj, M. Singh, *Ceram. Int.* **47**, 30902 (2021).
20. M. Raghasudha, D. Ravinder, P. Veerasomaiah, *SSP* **241**, 69 (2016).
21. K. Hussain, N. Amin, M.I. Arshad, *Ceram. Int.* **47**, 3401 (2021).

Дослідження ефекту заміни хрому церієм у феритах магнію на діелектричні та структурні властивості

Hamed A. Younis[1], Wissam A. Hussian[1], Omar A. Ahmed[1], Mustafa H. Omar[2]

[1] *The General Directorate for Education in Diyala, Diyala, Iraq*
[2] *Department of Materials Engineering, College of Engineering, University of Diyala, Diyala, Iraq*

Досліджено структурні та діелектричні властивості церій-хромового заміщення у фериті магнію ($x = 0$, 0.1, 0.3, 0.5), отриманому самозайманням лимонної кислоти та прожареному при температурі (1000 °C). Характеристику складу зразків проводили за допомогою XRD, FTIR, TEM, а діелектричні властивості вимірювали за допомогою LCR. Рентгенівська дифракція виявила склад кубічної шпінелі. Розмір кристала магнієвого фериту був у межах (18-31 нм) і постійної решітки (8,327-8,393 Å). Було помічено, що спектри FTIR сполуки $MgCr_{0.5-x}Ce_xFe_{1.5}O_4$ залишаються у шпінельній фазі зі зміною концентрації Ce^{3+}. Електронно-мікроскопічні вимірювання показали, що існують різні вершини решітки з потенційним d-розташуванням для Cr_2O_3, CeO_2 та α-Fe_2O_3 фази. Значення d-розташування найбільш помітного кільця в кристалічних площинах (311) $MgFe_2O_4$ було близьким до його значення в рентгенівській дифракції. Було встановлено, що діелектрична проникність і коефіцієнт діелектричних втрат зменшуються зі збільшенням частоти прикладеного електричного поля і змінної провідності.

Ключові слова: $MgFe_2O_4$, Діелектричні властивості, Золь-гель, ТЕМ, FTIR.